

A NANOFLUID ÁRAMLÁSÁNAK NUMERIKUS SZIMULÁLÁSA HULLÁLT CSATORNÁN KERESZTÜL ÖRVÉNYGENERÁTORRAL

NUMERICAL SIMULATION OF NANOFLUID FLOW THROUGH A CORRUGATED CHANNEL WITH VORTEX GENERATOR

Aimen TANOUGAST*, Krisztián HRICZÓ**

ABSTRACT

The radiator is an important part of a car. It cools the different parts of the vehicle by indirect heat exchange, by circulating coolant through the radiator. Heat transfer conditions are a function of the flow, geometry, and temperature characteristics. The present work concerns the numerical study of two-dimensional turbulent flow, with heat transfer in a corrugated channel with and without vortex generators, using Al₂O₃-water nanofluid as a heat transfer liquid.

The governing equations of the flow are the continuity equation, the momentum equation, and the energy equation modeling the heat transfer. This partial differential equation system was discretized and solved using the Ansys-Fluent commercial software based on the finite volume method. The standard k-ε model was used to model turbulence.

We analyzed the effect of parameters and the vortex generators on the solutions. The obtained results were presented graphically.

1. Introduction

An efficient heat exchange is often synonymous with increased performance, and the improvement of heat exchange in many industrial sectors requires the intensification of heat transfer by convection. To do this, a large number of researchers have conducted several numerical and experimental tests to increase the exchange surface. Others, on the other hand, have worked on heat transfer fluids, and the primary parameter that allows us to evaluate the potential of heat exchange is the thermal conductivity. The idea is then to disperse particles of nanometric size in the base fluid to increase its conductivity, hence the name of nanofluid. M. FIEBIG. [1] Published papers about the effect of Transverse and longitudinal vortex generators on heat transfer. Longitudinal vortices are more efficient for heat transfer enhancement than transverse vortices. Heat transfer enhancement increases with Reynolds number and increases for constant winglet aspect ratio with angle of attack up to a maximum angle of attack; but it

also increases up to limiting values for winglet height relative to transverse and streamwise winglet spacing and relative to boundary layer thickness.

S.Eiamsa-ard, P.Promvonge. [2] Have invested in an experimental study enhancement of heat transfer by means of helical tape inserts in a double pipe heat exchanger using cold water and hot air as the test fluids. Experimental results confirmed that enhanced heat transfer. The full-length helical tape with rod provides the highest heat transfer rate, about 10% better than that, without a rod. The pressure drop from the full-length helical tape insert decreases at low Reynolds numbers due to weak swirling flow but increases substantially at higher values of Reynolds numbers. The different free-spacing ratio value should be about unity for $Re < 4000$. The regularly spaced helical tape inserts at $s = 0.5$ yields the highest Nusselt number yield, which is about 50% above the plain tube.

M. Henze and all. [3] Have been experimentally investigated. The heat transfer and flow field using a transient method based on temperature measurement with thermochromic liquid crystals was used to obtain the heat transfer distribution behind a tetrahedral, full-body vortex generator. Turbulence promoters or vortex generators (VGs) are often used to manipulate the flow field and create turbulence. The heat transfer enhancement at different positions behind the VG is shown.

Veeranna Sridhara, Lakshmi Narayan Satapathy. [4] They published a review about nanofluids and the most important characteristics (kind and size of nanoparticles, volume fraction). These characteristics affect properties of the base fluid, increase the thermal conductivity, and viscosity. The Al₂O₃ nanoparticles varied in the range from 13 to 302 nm to prepare nanofluids, and the observed enhancement in the thermal conductivity was 2% to 36%.

S. R. Nfawa et al. [5] have numerically studied the turbulent flow in a trapezoidal corrugated channel with vortex generators for heat transfer enhancement. To achieve this objective, four amplitude heights were introduced: 1, 2, 3 and 4 mm. A constant heat flow is adopted as the thermal condition on the walls of the lower and upper corrugations, with a Reynolds number Re varying from 5000 to 17 500. The results found show, that in the case of the configurations with vortex

* PhD student, Institute of Mathematics, University of Miskolc

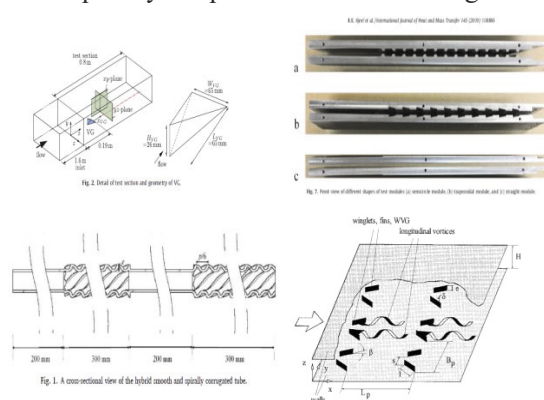
** associate professor, Institute of Mathematics, University of Miskolc

generators, a significant improvement of the Nu but accompanied by an increase of the friction coefficient is observed compared to the configuration without generators. Therefore, the vortex generator could be favorable in several heat transfer applications.

Raheem K. Ajeel and all. [6] They investigated the forced convective turbulent flow of SiO₂-water nanofluid through different corrugated channels being studied numerically and experimentally, using particle volume fractions (1% and 2%). The numerical results were close to the experimental results. It shows that the enhancement in heat transfer is due to corrugations and nanoparticles. The Nusselt number was increasing with Reynolds number. Corrugation creates a vortex, and the nanoparticles increase the conductivity of fluid, at the same time, the vortex and nanoparticles increase the friction, and this leads to a pressure drop.

Chen Yang and all. [7] Study the combination of the smooth part and the corrugated part, the effect of geometrical parameters on heat transfer, pressure loss; the heat transfer enhancement, while the maximum augmentation is found to be 258%. To evaluate the pressure loss of a hybrid, smooth, and spirally corrugated tube, the friction factor ratio is calculated with the comparison of smooth tubes. Results show that tube of the case with p/D ¼ 4.5 generates less pressure loss.

Filipe Neves and all. [8] Focuses on the numerical study of the performance of two nanofluids (Al₂O₃ water and TiO₂-water) in heat transfer by forced convection in a flat tube of an automobile radiator. Increasing the concentration of nanoparticles can improve the heat transfer characteristics of nanofluids. The use of alumina and titanium dioxide nanoparticles have a similar behavior regarding heat transfer. The utilization of nanofluids in the radiator of automobiles, enhances radiator performance, because the nanofluids can improve the processes related to heat transfer and consequently the performance of the engine.



1. figure some examples about corrugations and vortex generators

2. Mathematical formulation

The study of physical phenomenon is often formulated by laws expressed in the form of mathematical equations with partial derivatives which are elliptical and nonlinear on the one hand, and complex and coupled on the other hand, linking the various parameters, namely speed, pressure and temperature, which will be validated at each point of the field of study.

These equations obtained from the fundamental laws of mechanics and thermodynamics are:

- 1- The continuity equation, which translates the principle of conservation of mass.
- 2- The equations of Navier-Stokes which translate the principle of conservation of the quantity of movement.
- 3- The energy equation based on the first principle of thermodynamics.

2.1. General equations governing the flow

Simplifying assumptions

- An incompressible fluid ($\rho = \text{cte}$).
- A viscous Newtonian fluid ($\mu \neq 0$).
- Constant physical properties.
- Steady state ($\frac{\partial}{\partial t} = 0$).
- 2D ($\frac{\partial}{\partial x_3} = 0$ and $U_3 = 0$).
- Negligible volume forces.
- Turbulent flow.

Taking into account these simplifying assumptions (e.g. [8]), the general equations governing the flow and heat transfer become:

2.1.1 Continuity equation

$$\frac{\partial u_i}{\partial x_i} + \frac{\partial \bar{u}_i}{\partial x_i} = 0 \quad (1)$$

$$\frac{\partial \bar{u}_i}{\partial x_i} + \frac{\partial \bar{u}_i}{\partial x_i} = 0 \rightarrow \frac{\partial \bar{u}_i}{\partial x_i} = 0 \quad (2)$$

$$\frac{\partial \bar{u}_i}{\partial x_i} = 0 \quad (3)$$

2.1.2- Equation of momentum

$$\frac{\partial(\bar{u}_i \bar{u}_j)}{\partial x_j} + \frac{\partial(\bar{u}_i \bar{u}_j)}{\partial x_j} = -\frac{1}{\rho} \frac{\partial \bar{P}}{\partial x_i} + \nu \frac{\partial}{\partial x_i} \left(\frac{\partial \bar{u}_i}{\partial x_j} + \frac{\partial \bar{u}_j}{\partial x_i} \right) \quad (4)$$

$$\frac{\partial(\bar{u}_i \bar{u}_j)}{\partial x_j} = -\frac{1}{\rho} \frac{\partial \bar{P}}{\partial x_i} + \frac{\partial}{\partial x_j} \left(\nu \left(\frac{\partial \bar{u}_i}{\partial x_j} + \frac{\partial \bar{u}_j}{\partial x_i} \right) - \bar{u}_i \bar{u}_j \right) \quad (5)$$

2.1.3 Energy equation

$$\frac{\partial(\rho C_p U_j \bar{T})}{\partial x_j} = \frac{\partial}{\partial x_j} \left(K \frac{\partial T}{\partial x_j} - \rho C_p \overline{u_j \bar{T}} \right) \quad (6)$$

2.2 k-epsilon model

The k-epsilon model is a two-equation model that gives a general description of turbulence using two transport equations, one for turbulent kinetic energy (k) and the other for dissipation (epsilon). The turbulent dissipation is the rate at which velocity fluctuations dissipate. This model uses the Boussinesq concept, based on the analogy between the exchange of momentum by molecular interaction at the microscopic scale and the exchange of momentum by turbulence at the macroscopic scale. The k-ε model uses the gradient diffusion assumption to relate Reynolds stresses to mean velocity gradients and turbulent viscosity.

$$-\overline{u_i u_j} = \nu_t \left(\frac{\partial \overline{u_i}}{\partial x_j} + \frac{\partial \overline{u_j}}{\partial x_i} \right) - \frac{2}{3} k \delta_{ij} \quad (7)$$

2.2.1 Turbulent kinetic energy transport equation

$$\frac{\partial \rho}{\partial x_i} (\rho k U_j) = \frac{\partial}{\partial x_i} \left[\left(\mu + \frac{\mu_t}{\sigma_k} \right) \frac{\partial \epsilon}{\partial x_j} \right] + G_k - \rho \epsilon \quad (8)$$

2.2.2 Transport equation for the dissipation rate ε of turbulent kinetic energy

$$\frac{\partial \rho}{\partial x_i} (\rho k U_j) = \frac{\partial}{\partial x_i} \left[\left(\mu + \frac{\mu_t}{\sigma_\epsilon} \right) \frac{\partial \epsilon}{\partial x_j} \right] + C_{1\epsilon} \left(\frac{\epsilon}{k} \right) G_k -$$

$$C_{2\epsilon} \rho \frac{\epsilon^2}{k} \quad (9)$$

$$G_k = -\rho \overline{U_i' U_j'} \frac{\partial \overline{U_j}}{\partial x_i} = \rho \nu_t \left[\frac{\partial \overline{U_i}}{\partial x_j} + \frac{\partial \overline{U_j}}{\partial x_i} \right] \frac{\partial \overline{U_i}}{\partial x_j} \quad (10)$$

2.3 Calculation of the thermo-physical properties of the nanofluid

The thermo-physical properties of the nano fluid AL_2O_3 are calculated from the following equations:

- Effective Density

$$\rho_{nf} = (1 - \Phi) \rho_f + \Phi \rho_p \quad (11)$$

- The volume fraction

$$\Phi = \frac{\text{solid volume nanoparticle}}{\text{total volume of the nanofluid}} = \frac{v_p}{v_f + v_p} \quad (12)$$

- Effective specific heat (Xuan and Roetzel correlation)

$$(\rho C_p)_{nf} = (1 - \Phi) (\rho C_p)_f + \Phi (\rho C_p)_p \quad (13)$$

- Effective dynamic viscosity (Corcione correlation)

$$\frac{\mu_{nf}}{\mu_f} = \frac{1}{1 - 34.87 \left(\frac{d_p}{d_f} \right)^{-0.3} \Phi^{1.03}} \quad (14)$$

- Effective thermal conductivity (Maxwell's correlation)

$$\frac{k_{nf}}{k_f} = \frac{k_p + 2k_f + 2(k_p - k_f)\Phi}{k_p + 2k_f - (k_p - k_f)\Phi} \quad (15)$$

The properties are determined from the properties of water and the AL_2O_3 at 298 K, with a fraction $\Phi = 3\%$

1. Table. Thermo-physical properties of the base fluid water and the nanoparticle AL_2O_3 .

	Water	AL_2O_3
ρ (kg/m ³)	998.2	3600
C_p (J/kg.°K)	4182	765
K (W/m.°K)	0.6	36
μ (kg/m.s)	0.001003	-

2.4 Adimensional numbers

Reynolds Number:

$$Re = \frac{\rho \cdot u \cdot D_h}{\mu} \quad (16)$$

Nusselt number:

$$Nu = \frac{h \cdot Lc}{\lambda} \quad (17)$$

Coefficient of friction:

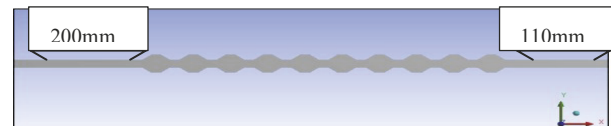
$$C_f = \frac{\tau_w}{0.5 \cdot \rho \cdot u^2} \quad (18)$$

Coefficient of thermal performance:

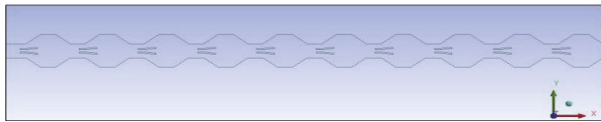
$$PEC = \frac{\left(\frac{Nu_{moy}}{Nu_{moy,ref}} \right)}{\left(\frac{f}{f_{ref}} \right)^{1/3}} \quad (19)$$

3. Numerical Modeling

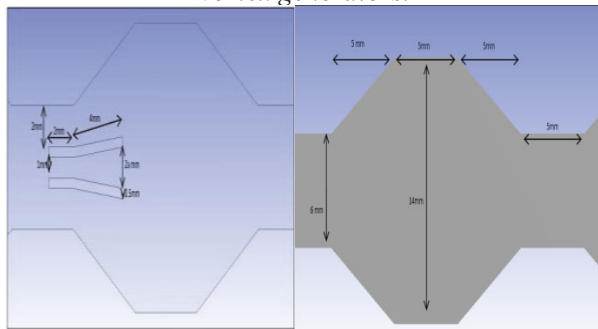
In the following, the different geometries, the generation of their mesh and the incorporation of boundary conditions as developed in the Ansys-Fluent preprocessor are described.



2. Figure Geometry without vortex generators.



3. Figure Central part showing the corrugations with vortex generators.



4. Figure Different dimensions on vortex generator and corrugation

The boundary types of the geometries considered in this work are summarized in the table below.

2. Table Types of boundaries.

Region	Type
Input	Velocity
Output	Pressure
Wall (smooth channel)	Adiabatic
Wall (corrugations)	Heat flow
Vortex generator	Adiabatic

4. Results and Discussion

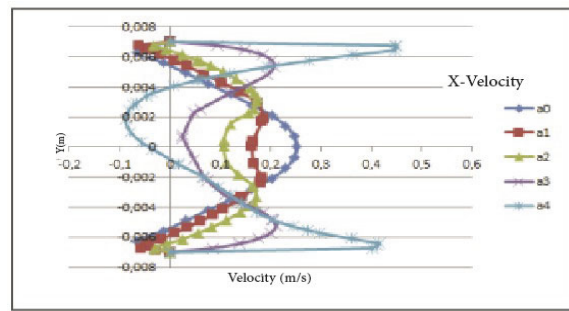
4.1 Effect of the Grid:

Figures (5) below, represent, the pressure and velocity profiles at a position $x=287.5\text{mm}$ and y vary from -7 to $+7\text{mm}$. The different curves were obtained with meshes made of 9141, 12883, 37191 and 55302 nodes for a Reynolds number of 17500.

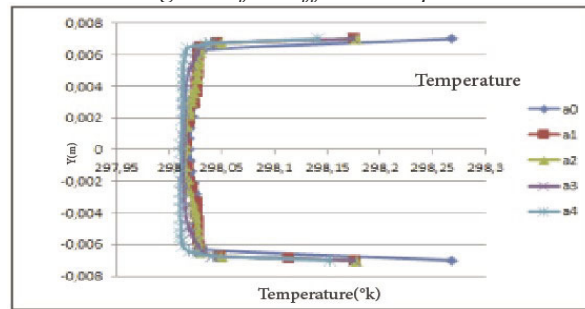
5. Figure Pressure and Velocity profile on a line at the 5th corrugation.

4.2 Numerical Simulation:

Figure (6) represents the velocity profile on a line from $[-7\text{mm}$ to $7\text{mm}]$ in the middle of the 5th corrugation with a vortex generator and this for different amplitudes. We notice that the velocity was parabolic in the middle and changes direction until it became negative under the effect of the vortex generator. Also, on figure (7), we notice that the temperature increases significantly with the increase of the amplitude.

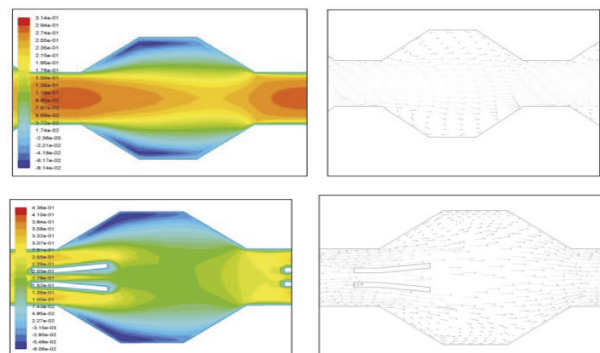


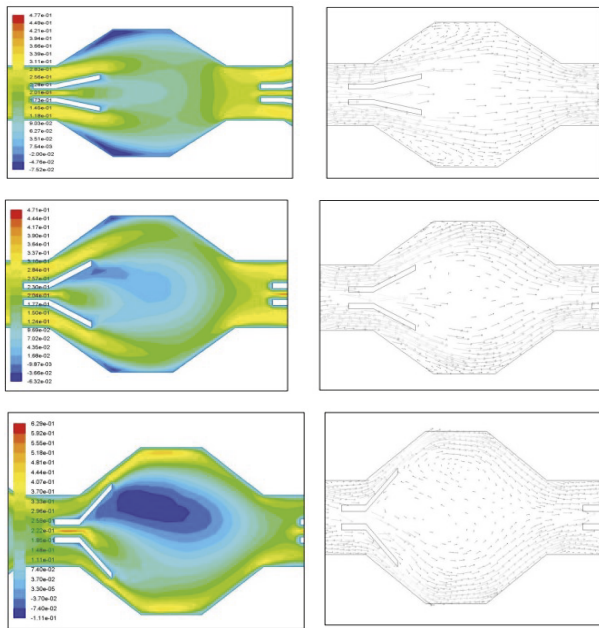
6. Figure Velocity profile on a line at the 5th corrugation for different amplitudes



7. Figure Temperature profile on a line at the 5th corrugation for different amplitudes

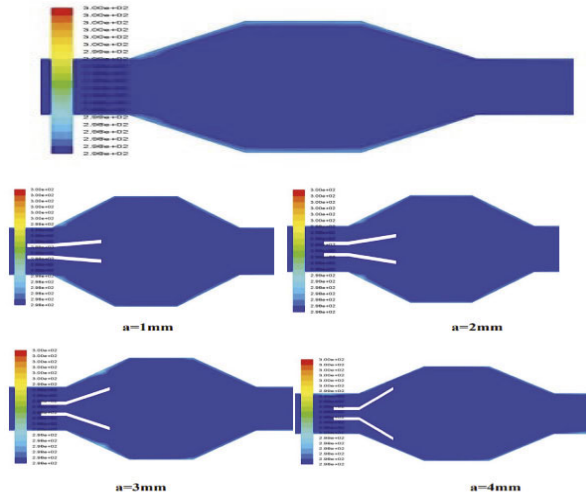
Figures (8) represent the contours and velocity vectors for a Reynolds number equal to 5000 with and without vortex generators. In the case of corrugations without vortex generators, an acceleration of the fluid is noted at the central section of the channel, and which weakens as one moves away from and towards the wall. On the other hand, in the case of corrugations with vortex generators, and each time the amplitude increases, there is elimination of the stagnation zone of the fluid at the wall, to go to concentrate in the middle. Moreover, this behavior is confirmed by the recirculation zones on the figures of the speed vectors. At the level of the upper and lower walls, the behavior is almost identical.





8. Figure Contour and velocity vector with and without vortex generators.

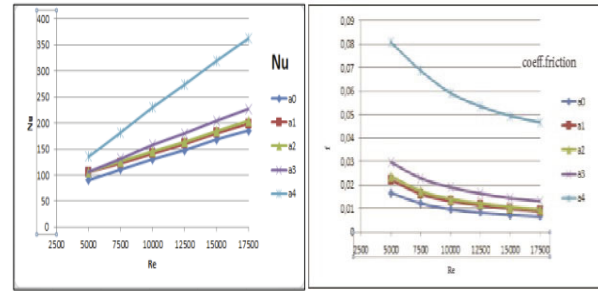
Figures (9) show the temperature contours for a Reynolds number of 5000 with and without vortex generators. It is clear that the vortex generators have a great influence on the temperature gradient in the walls; as the amplitude of the vortex generators increases, the thermal boundary layer becomes thinner and the heat transfer is better.



9. Figure Temperature contours (Re=5000)

Figures (10) represent, the variation of the Nusselt number and the friction coefficient as a function of the Reynolds number without and with vortex generators at different amplitudes. It can be seen that the Reynolds number and the amplitude have a significant influence on the Nusselt number. The latter increases with the increase of the amplitude, so the heat transfer is better. Also, the friction coefficient increases contrary to what

it should be because the velocity gradient is important at the wall.



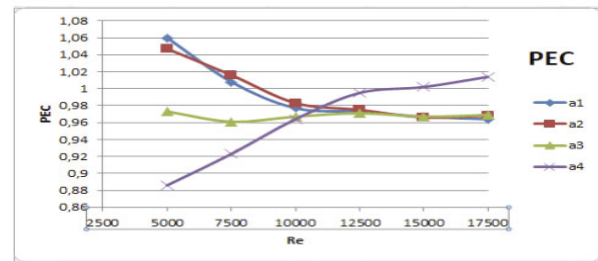
10. Figure Variation of the Nusselt number and friction coefficient as a function of the Reynolds number

Figure (11) represents the performance criterion PEC, which represents here the ratio of the Nusselt of the corrugations with the generator to that without the vortex generator to the friction of the corrugations with the generator to that without the vortex generator:

$$PEC = \frac{(N_{GV}/N_{SGV})}{(f_{GV}/f_{SGV})^{1/3}}$$

GV; SGV: it mean with and without vortex generators respectively.

We notice that this factor increases with the increase of Reynolds number until reaching a value of 1 for an amplitude of 4mm, so it is an optimal amplitude which is chosen to pass to the second part of study, that of the nanofluid.



11. Figure Variation of the performance criterion as a function of the Reynolds number.

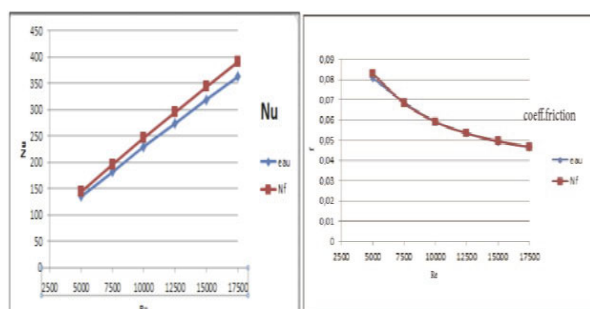
4.3 Comparison between: base fluid (water) and nanofluid (Al₂O₃ / water):

In the following results for the studied configuration with vortex generators (amplitude = 4 mm) using the base fluid (water), the nanofluid (Al₂O₃ / water) will be shown.

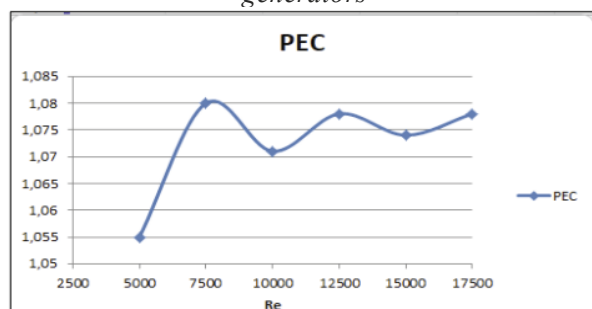
Figure (12;13) shows the variation of the Nusselt number, the friction coefficient as well as the performance criterion as a function of the Reynolds

number, with vortex generators. It can be seen that the Nusselt number increases significantly with increasing Reynolds number, with larger values for the Al₂O₃ / water nanofluid compared to pure water, which is in favor of improved heat transfer.

Moreover, the coefficient of friction results for both fluids used are identical, which means that nanoparticles have no effect on the coefficient of friction. Also, the PEC is around 1 (figure 13), which clearly shows that the nanofluid is much better than pure water, in favor of an improvement of the heat transfer.



12. Figure Variation of the Nusselt number and the friction coefficient as a function of Reynolds. For water and Al₂O₃ / water ($\phi = 3\%$) With vortex generators



13. Figure Variation of PEC as a function of Reynolds. With vortex generators

5. CONCLUSION

The numerical study of the turbulent flow of a nanofluid through a corrugated channel with a trapezoidal base with and without vortex generators was the objective of the present work.

Initially, the basic fluid flow (water) without vortex generators was studied and then the flow with vortex generators at different amplitudes was considered.

This study reveals:

- The effect of Reynolds number on the thermal and dynamic fields.
- The increase of the amplitude of the vortex generators leads to the increase in pressure.
- In the case of corrugations with vortex generators, each time the amplitude increases,

there is an elimination of the stagnation zone of the fluid at the wall, to be concentrated in the middle of the channel.

- As the amplitude of the vortex generators increases, the thermal boundary layer becomes thinner, and the heat transfer is better.
- The Reynolds number and the amplitude have a significant influence on the Nusselt number, but the friction coefficient increases contrary to what it should be.
- The PEC factor increases with increasing Reynolds number until it reaches a value of 1 for an optimal amplitude of 4mm.
- The Nusselt number values are higher for the Al₂O₃ / water nanofluid than for pure water.

The nanoparticles have no effect on the friction coefficient.

6. REFERENCES

- [1] M. FIEBIG. VORTICES, GENERATORS AND HEAT TRANSFER. Trans IChemE, Vol 76 18 September 1997.
- [2] S.Eiamsa-ard, P.Promvong. Enhancement of heat transfer in a tube with regularly-spaced helical tape swirl generators. Solar Energy pages 483–494, 29 September 2004.
- [3] M. Henze , J. von Wolfersdorf, B. Weigand, C.F. Dietz, S.O. Neumann. Flow and heat transfer characteristics behind vortex generators – A benchmark dataset, International Journal of Heat and Fluid Flow pages 318–328. 14 July 2010.
- [4] Veeranna Sridhara, Lakshmi Narayan Satapathy. Al₂O₃-based nanofluids: a review. Nanoscale Research Letters 456, 16 July 2011.
- [5] S.R.Nfawa, A.R.A.Talib, S.U.Masuri, A.A.Basri, H.Hasini. Heat Transfer Enhancement in A Corrugated-Trapezoidal Channel Using Winglet Vortex Generators, CFD Letters 11, Issue 10, pages 69-80, 2019.
- [6] Raheem K. Ajeel, W.S.-I. Salim and all. Turbulent convective heat transfer of silica oxide nanofluid through corrugated channels: An experimental and numerical study. International Journal of Heat and Mass Transfer pages 145.28 September 2019.
- [7] Chen Yang and all. Thermohydraulic analysis of hybrid smooth and spirally corrugated tubes. International Journal of Thermal Sciences pages 158.2020.
- [8] Filipe Neves and all. Forced convection heat transfer of nanofluids in turbulent flow in a flat tube of an automobile radiator. Energy Reports pages 1185-1195, 19 July 2022.